International Journal of Science and Technology Education Research Vol. 1(6), pp. 132 - 142, November 2010
Available online http://www.academicjournals.org/IJSTER
ISSN 2141-6559 ©2010 Academic Journals

Full Length Research Paper

High concentration ozone generation in the laboratory for various applications

T. Vijayan* and Jagadish G. Patil

Pillai's Institute of Information Technology, Engineering, Media Studies and Research (PIIT) Dr. K. M. Vasudevan Pillai's Campus, Sector 16, New Panvel, Navi Mumbai - 410 206, India.

Accepted 21 September, 2010

Ozone (O_3) the allotrope of oxygen is a powerful disinfectant and oxidant and nature's agent for cleansing the environment. Ozone present in nature is only of sub-ppm level. In order to have ozone in large quantities, it is inevitable that same is produced artificially in a machine. In our laboratory, we have devised a novel and innovative plasma device for forming ozone in large quantities of thousands of ppm in oxygen corona discharge. This ozone is useful for various applications, such as, purification of ambient air and potable water, disinfecting food products to increase shelf life, ozone therapy, fumigation of operation theaters in hospitals, sterilization of operation tools and personnel, etc. Applications related to environment protection enjoy carbon credits. In the plasma device of axial symmetry, oxygen corona plasma is formed in between a novel cathode (K) and anode (A) of the diode in which a high electric field around 1-10 MV/m enhanced the corona plasma density. Electrons energized by the electric field collided with the background O_2 which then split into O radicals. The radicals in turn joined other free O_2 molecules and formed O_3. The corona formation and O_3 genesis in this ozone generator are modeled and investigated. Electrons in plume multiplied through primary and secondary ionizations and for typical diode geometry with A-K gap d=10 mm and potential 10 kV resulted in electron densities over 10^{14}-10^{15} m^{-3}. This in a cold corona formed in gas pressure in thousands of Torr and wide gaps 10 - 30 mm favored formation of ozone densities over 10^{19} m^{-3}. Ozone output as required in different applications is controlled by varying the voltage and current in diode in a range suitable for negligible Joule heating which inhibited ozone genesis. Preliminary experiments on the generator so developed, gave ozone concentrations in hundreds of ppm.

Key words: Modeling, innovative diode, electron emission, avalanche multiplication, poisson field, cold corona plasma, ozone generation, development, experiments, ozone measurements.

INTRODUCTION

Ozone (O_3) the allotrope of oxygen is a powerful disinfectant and oxidant and so applied in various important applications such as purification of ambient air and potable water (Kogelschatzt et al., 1999; Renner et al., 1988), disinfecting food products to increase shelf life; fumigation of operation theaters in hospitals, sterilization of operation tools and personnel; ozone therapy (Vijayan and Patil, 2008), etc. As a disinfectant, it is a much more powerful and effective than the much used chlorine which escapes to atmosphere as a pollutant and is toxic. Chlorine is used in practice as it is less expensive compared to ozone and the more powerful radical, hydroxide (OH).

Ozone is the nature's way of cleansing the environment of polluting gases and protects life on earth from global warming. Ozone present in environment is of sub-ppm level and is mainly formed by irradiation of the oxygen molecules by ultraviolet (UV) radiation in sunlight. Oxygen molecule (O_2) is split into atomic radicals O and O^- and is described by Equation (1) for the case of electron irradiation. Alongside the radicals combine with free molecules O_2 and form O_3. These processes are described by Equations (1) and (2) and conceptualized in Figure 1.

*Corresponding author. E-mail: vijayan.tvijay@gmail.com.

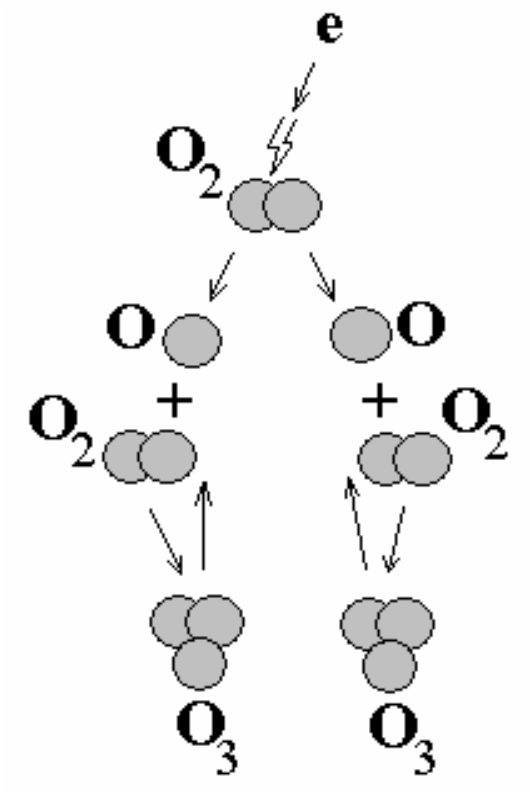

Figure 1. Ozone formation and reversal processes.

$$e + O_2 \longleftrightarrow O + O + e \quad (1)$$

$$2O_2 + O \longleftrightarrow O_3 + O_2 \quad (2)$$

The processes are reversible and have half-lives of only tens of minutes at the ambient temperature.

In nature, the ozone layer that is formed at the lower pressures and encircles the earth over the outer atmosphere has higher concentrations over ppm. This layer protects life on earth from the penetrating UV radiations as well as from global warming. Apart from this, ozone of higher concentrations of order ppm is also formed quite readily in nature during lightning strikes and thunderstorms. First rainfall washes the ozone in atmosphere to the ground and causes overnight green sprouts that cover the ground as a result of rapid germination and plant growth. The fresh, clean, spring rain smell that we experience after a storm is also due to the presence of naturally created ozone. Similarly, ozone is created by water falls due to frictional forces, shocks and other violent natural impulses.

Ozone is highly reactive as it is radical and unstable. It so oxidizes and decomposes wastes in the surroundings, and turns them in to harmless products. In congested urban areas where a lot of industrial chemicals are spewed into the atmosphere and the pollutant levels are high, UV rays from sun irradiate them and produce ozone. This ozone in turn tends to oxidize and reduces the chemicals in air and wastes in land fills. Similarly when ozone is admitted inside a room it purifies the air, removes odor and freshens air with fragrance (Kogelschatzt et al., 1999). The use of ozone leaves no toxic by-products or residues of its own and is non-carcinogenic. Applications related to environment protection from green house gas emission responsible for pollution and global warming, enjoy carbon credits. As noted, ozone concentrations in nature are at low level whereas many of the applications cited above need ozone in high concentrations and in controlled conditions which can be produced only artificially in a generator. Control and regulation of process and concentration are also attained then. Ozone is produced in laboratory in a number of ways (Jen-Shih Chang, 1991; Kitayama and Kuzumoto, 1997; Yagi and Tanaka, 1979; Dekowski et al., 2004) such as, by using UV irradiation, by high frequency (hf) corona discharge, by high voltage (HV) corona discharge, etc. Of these, corona plasma discharge route of ozone generation is found to be highly efficient (Kogelschatzt et al., 1999; Jen-Shih Chang, 1991). Maximum O_3 formation about 20% in pure oxygen pressure ~ 10^3 Torr has been reported. In this method, oxygen gas is filled in between the cathode and anode of a diode (Vijayan, 2006) and suitable voltage is applied across the electrodes, formed a cold corona discharge over the cathode surface. Evolution of ozone takes place in this corona plasma. For given diode geometry, the voltage, current and gas pressure are suitably tuned to obtain a right corona discharge for maximizing ozone production. Since, ozone-life reduces sharply with rise in temperature, Joule heating of corona is avoided by restricting the discharge currents in diode (Yagi and Tanaka, 1979; Dekowski et al., 2004; Pekarek et al., 2000). As cited earlier, O_3 is short lived and reverts rapidly to O_2. So, most of applications with ozone are conducted *in situ* or close to its generation point.

This paper theoretically investigates the electric field induced corona plasma formation in ozone generator diode. A model of corona plasma formation leading to ozone genesis applied to various geometries is described, and results are discussed. Since voltage breakdown in medium gives rise to infinite current and Joule heating which does not favor ozone genesis, is not covered in this study. As said above, ozone is a strong disinfectant and sterilizer. For sterilizing the room air in a dynamic state, the ozone dosage allowed is only around 0.02 - 0.04 ppm. However, for fumigating operation theaters and wards in hospitals, higher dosages in tens of ppm are generally applied in closed room conditions where personnel are not present. This is necessary for destroying the many types of harmful bacteria and germs. After fumigation the room is closed for longer time so that the ozone level drops to acceptable level. Similarly ozone is used for sterilization of operation tools and personnel.

Safe dosage in bottled water ready for consumption is around 0.1 - 0.4 ppm. However, extremely high dosages in tens of ppm are used during its purification process. Since ozone decays fast, the processed water is fit for consumption within a short time and allays any safety concerns. Ozone is also used for purifying water in swimming pools with ozone concentration around 0.05 - 0.1ppm. Ozone bubbled in warm baths/showers provides stimulation of local circulation and disinfectant action in human body.

Ozone therapy is used in general under controlled dosages by doctors for treatment of many ailments. Prevention and cure of many communicable diseases viz. mumps, measles, influenza, cholera, tropical fevers, etc. are observed. For treating cancer, ozone therapy combined with chemotherapy has been routinely applied. Ozone dosages 0.3 – 0.8 ppm are used for inhibition of cancer cell growth. Also, ozone is useful for reinforcing the body massage oil for their antibacterial properties as well as their healing properties. Ozonated oils are formed by bubbling high ozone concentrations through them. Ozonated oils hold the ozone almost indefinitely as compared to a few minutes in ozonated water. Ozonated olive oil is ideally suited for healing wounds that would not heal otherwise. It not only kills bacteria, fungus, and other pathogens thereby sterilizing the wound, but also stimulates healing. Ozonated coconut oil known as cocozone is useful for many applications such as relieving vaginal thrush, athlete's foot, ringworm, fungus on skin/fingernails and also as a disinfectant for wounds, burns, cuts, etc. Ozone mixed in detergent and toilet soaps could yield better cleaning and hygiene.

Ozone is also used for food preservation whereby extension of shelf-life renders to less food wastage. For this the food to be processed is stored in a closed chamber and treated with ozone concentration of a few ppm. As ozone is a strong oxidizing agent, it is used for bleaching fabrics and similar materials as well.

OZONE GENERATOR AND PROCESSOR DETAILS

The ozone generator cum processor which has been developed in our laboratory is schematically shown in Figure 2a. Details of the main components of the system (Vijayan, 2006) are thus described. The novel and innovative diode geometry of axial symmetry is illustrated in Figure 2b and is also represented by its symmetric half-plane about the axis in Figure 3.

Plasma diode geometry

The ozone generator contains the plasma diode which has cylindrical geometry with cathode (K) coaxially surrounded by an anode cup (A) and separated by annular A-K gap d across which a voltage ϕ_0 is applied from a high voltage (HV) supply. The cathode is made of a large number (up to 192) of sharpened nozzles assembled on various radial planes on the axial cathode mast and connected to the negative terminal which is electrical ground of HV supply. The nozzles surrounded by the anode cup, in addition to creating high electric field close to the nozzle pinnacles, admits oxygen in to the A-K gap giving added novelty to present diode design. In order to maintain the purity of O_2, the diode region is initially evacuated to 0.001 Torr by using the vacuum pump shown in Figure 2a.

In the diode in Figures 2 to 3, there are 4 radial planes each containing 16 nozzles, totaling 64 nozzles in all. High electric field created by the cathode pinnacles causes field emissions and forms a negative corona discharge over cathode surface. The corona plasma when transiently formed covers only the cathode surface initially and thereafter tends to expand towards the anode. And when it completely fills the A-K gap could lead to a breakdown which however, is not of any interest in present study. The coronal plasma preceding the breakdown is of most significance for growing ozone and studied here.

As seen in Figures 2a and b; anode is floating at the positive potential and is insulated from the system ground by holding it on a HV Teflon bushing. It is connected to the HV power supply using a shielded coaxial HV cable. Overall HV electrical shielding of the generator is made complete with a shield dome covering HV Teflon bushing. All shielding and the generator vessel are connected to the common electrical ground for ensuring safe and user friendly operations. The cathode, anode, the generator vessel, and all metal parts which are in contact with ozone are made of the most ozone resistant metal, viz. stainless steel (SS-316). All other components in contact with ozone are made of ozone resistant materials, such as, Teflon. More details of the system are available elsewhere (Vijayan and Patil, 2008).

Ozone processor

Figure 2a also shows details of the processor unit meant for various ozone applications. We consider here first the processor for water purification. Ozone generated in the generator is led into a rectangular shaped reactor tank where water is processed and purified for human consumption. Provisions for purifying either tap water or pond water are available in Figure 2a. Prior to processing, water is filtered of the solid impurities of µm size and above and then collected in the water circulator tank. This water is pumped into a venturi line where it is first mixed with the ozone which is injected from the perpendicular line. The mixture is then led in to the reactor tank. Ozone is only partly dissolved in water in the process. In order to make more homogeneous mixing of ozone, water from venturi is forced through a diffuser

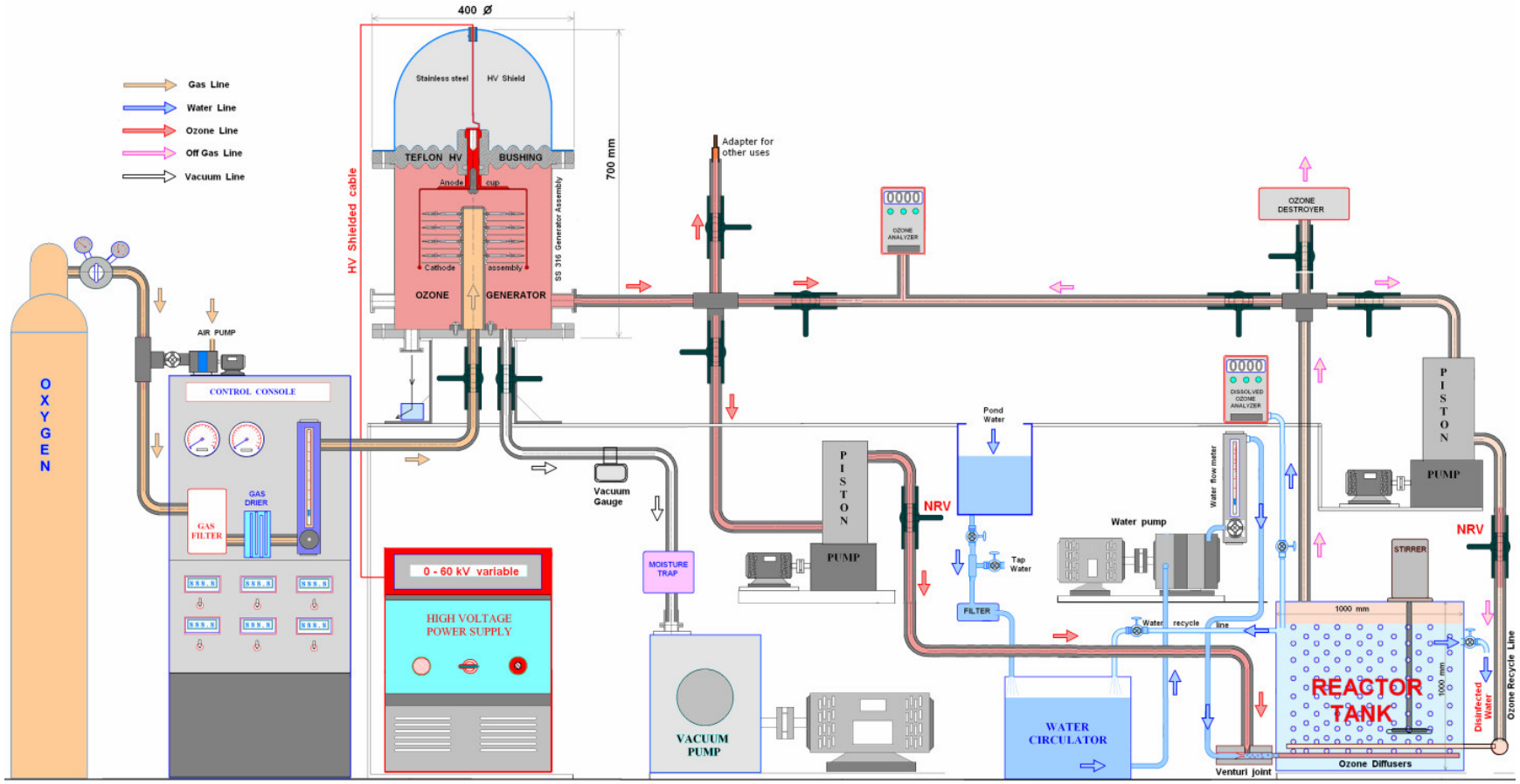

Figure 2a. Schematic of corona-plasma ozone-generator cum processing unit.

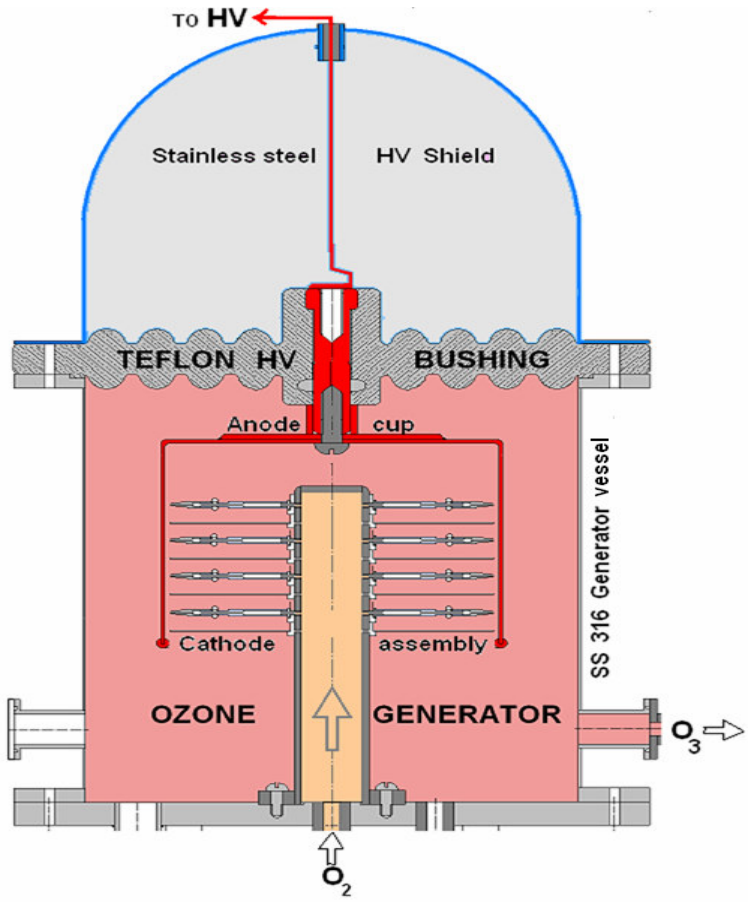

Figure 2b. Corona-plasma ozone-generator scheme.

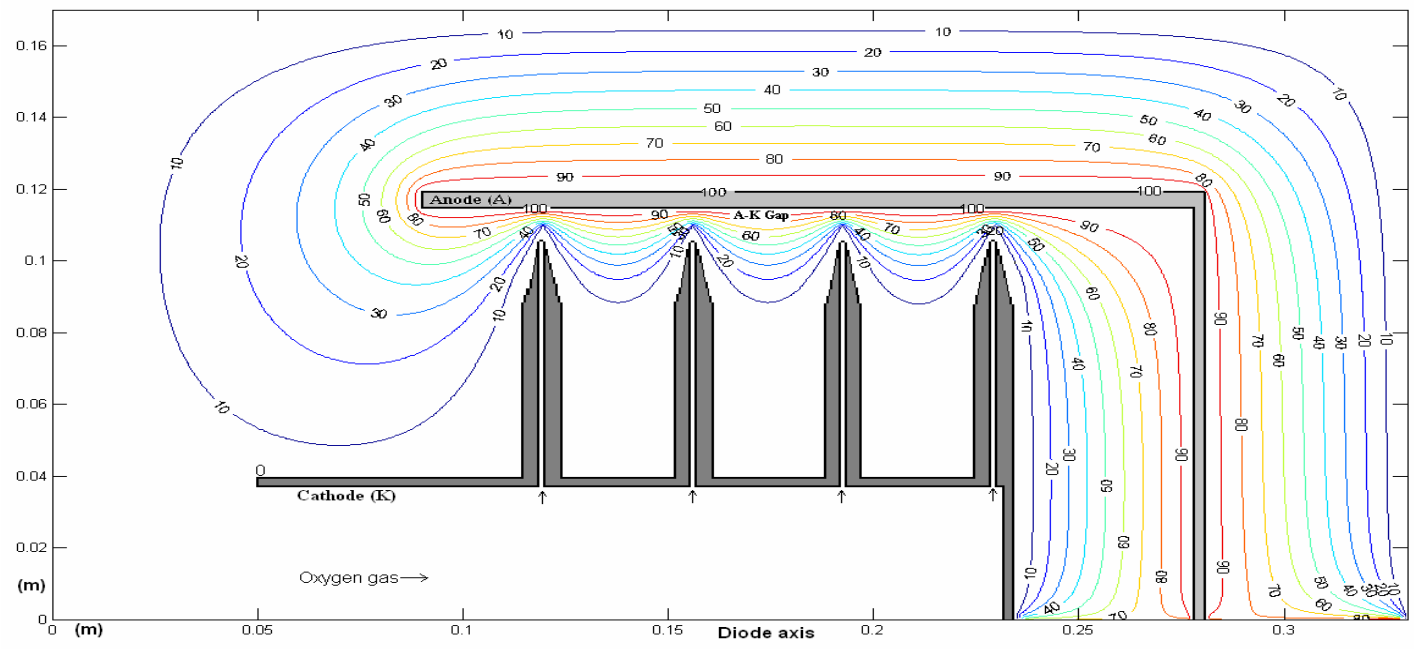

Figure 3. Plasma-diode geometry with cathode having 4-radial nozzle planes shown is the r-z symmetric section on one side of axis. Computed potential map for A- K gap d = 10 mm is also plotted in the figure.

line laid inside the reactor tank. Mixing is further improved by stirring the water with a motor driven stirrer suspended from tank top. The un-dissolved part of ozone which collects over the water surface in reactor tank is re-circulated by pumping it back to the reactor through a second diffuser on the ozone recycle line. For improving the degree of water purity still further, the processed water in reactor vessel is recycled and reprocessed. For this, the circulator tank is emptied of input water and filled with the processed water and processing as mentioned above repeated till the required purity is attained. Presently the ozone generator is being characterized in various conditions. Experiments of applications are expected to be taken up soon. For conducting experiments of other applications, an adapter provision is provided on the system in Figure 2a where the adapter can be attached to the chosen application module as desired.

The measurements of ozone produced in the generator and that collected above water surface in the reactor are done by the ozone analyzer shown next to the generator in Figure 2a. These are coordinated by selecting suitable isolation valves on the line. Ozone dissolved in water is measured by the dissolved ozone analyzer attached to the reactor tank. When the level of ozone measured over the water level inside the reactor is around a ppm it is led in to the ozone destroyer to reduce the dosage below 0.01 ppm before it is let off to the atmosphere. This is done as a safety precaution in order to avoid any toxic effect to the living beings.

MODELING OF CORONA FOR OZONE GENESIS

This section describes the theoretical formulations and modeling of corona and ozone genesis, and discusses the results obtained from the computations.

Theoretical formulations

Potential (ϕ) and electric field (E) distributions inside the A-K gap of the generator diode are described by the Poisson equation in axial symmetry (r,z) coordinates as:

$$\frac{d^2\phi}{dr^2}+\frac{1}{r}\frac{d\phi}{dr}+\frac{d^2\phi}{dz^2}=-\frac{\rho}{\varepsilon} \quad (3)$$

Where ρ is space charge density, permittivity $\varepsilon=\varepsilon_r\varepsilon_0$, ε_r is relative permittivity of oxygen gas, and ε_0 is permittivity of free space. ρ here is initially zero but assumes a finite value with onset of electron current. Electric fields in the given situations along the two co-ordinates are given from (3) as:

$$E_r=\frac{d\phi}{dr}\quad E_z=\frac{d\phi}{dz} \quad (4)$$

High electric field around the cathode tips induced field emission (FE) in durations of sub-picoseconds and corresponding current I_F (Vijayan and Patil, 2008) is given as:

$$I_F=2\pi r_K lf A_F\frac{E_r^{\,2}}{\varphi}\exp\left(\frac{-c_F\varphi^{3/2}}{E_r}\right) \quad (5)$$

Where A_F and c_F are FE constants, φ is work function of cathode (Kireeff Covo et al., 2006), r_K, l, f are cathode emitter radius, cathode length, and a factor describing the effective emission area. I_F in turn heated the cathode tips and initiated thermionic emission in times of picoseconds. The emissions hereafter are sustained by both the field (E_r) and temperature (T) and T-F emission current (Vijayan and Patil, 2008) so produced is:

$$I_{TF}=2\pi A_T T^2\exp\left(-e\varphi/k_B T\right)r_K lf\exp\left(\frac{c_T E_r^{1/2}}{T}\right) \quad (6)$$

Where A_T is thermionic constant, e is electronic charge, k_B is Boltzmann constant and c_T is T-F constant. Spatial ρ now on in continuity Equation (3) takes a finite value equal to:

$$\rho=\frac{J}{v} \quad (7)$$

$$J=\frac{I}{2\pi rl} \quad (8)$$

v is electron velocity, I is gas-collision inhibited spatial current driven by E_r and r is radial distance from cathode. ρ obtained from Equation (7) is used then in numerical solution of (3) to get ϕ, E_z and E_r at any point.

Electrons energized by E_r collide with O_2 molecules and dissociate them into free radicals O. Alongside ionization of the particles also takes place and the electron density (n_e) in gas medium increases to:

$$n_e=n_0\exp(\alpha r) \quad (9)$$

Where n_0 is initial electron density at cathode and α is Townsend first coefficient. The ions produced are accelerated in the opposite direction and strike and create secondary electrons from cathode. The electrons

tend to multiply n_e even more which is written as:

$$n_e = \frac{n_0 \exp(\alpha r)}{G} \quad (10)$$

Where,

$$G = 1 - \gamma[\exp(\alpha r) - 1] \quad (11)$$

and γ is Townsend second coefficient. For conditions of G=0, n_e is infinite causes electrical breakdown which is not desired here. Equation (10) in condition $\gamma[\exp(\alpha r) - 1] = 0$ is same as (9) and describes the corona plume covering cathode surface where only primary ionizations are active. Whereas, when γ is finite so that $1 > \gamma[\exp(\alpha r) - 1] > 0$, n_e is much larger than (9). In these conditions the corona expands to the anode till a stage when electron and its energy are fully lost in gas collisions.

Meanwhile free-radicals O in the medium combine with the free O_2 molecules and form ozone. For large electron energy $e\phi_0$, the ozone density (n_{oz}) so produced could be a few orders higher than n_e where total electron energy is fully utilized for O_3 producing collisions in a cold plasma. Q the energy for each O_3 genesis here is made of half of Q (O_2) the energy for dissociation of O_2 and Q (O_3) the energy of O_3 formation. That is:

$$Q = \frac{1}{2} Q(O_2) + Q(O_3) \quad (12)$$

As noted in Equations (1)-(2), radical O_3 revert back to O_2 and O with time. Inter molecular collisions aid O_3 decay and its density with time t reduces as:

$$n_t = n_{oz} \exp(-\lambda t) \quad (13)$$

Which has a half-life

$$t_{1/2} = \frac{0.5 n_{oz}}{\lambda} \quad (14)$$

Where t is in hours, n_{oz} is initial ozone density and the decay rate constant $\lambda = \frac{\ln(2)}{t_{1/2}}$ suitably averaged with (14).

The density reduces with temperature rise as well and is given as:

$$n_T = n_{T0} \exp(m\Delta T) \quad (15)$$

Where n_{T0} is density at temperature T_0 and $m = \frac{1}{n_{T0}} \frac{\partial n}{\partial T}$

Simulation model - computational studies

For the present axially symmetric diode geometry, Poisson's Equation (3) is written in a five-point matrix r-z finite difference (Vijayan and Venkatramani, 2004; Vijayan 1999) form as:

$$\phi_{r,z} = [\phi_{r,z+h} + \phi_{r,z-h} + (1 + h/2r)\phi_{r+h,z} + (1 - h/2r)\phi_{r-h,z} + h^2\rho/\varepsilon]/4 \quad (16)$$

Equation (16) was solved by employing MATLAB (Lyshevsk, 2003; Davis et al., 2007) in a matrix having 660 x 340 nodes with mesh step h=0.0005 mm. A successive over-relaxation method with a relaxation factor (ω) of 1.8 was used to iteratively solve the potentials at each node point. The potential relaxations converged to 1 x 10^{-6} percent in about 3000 iteration cycles.

From the converged potential map in the A-K gap the electric field at each node was determined as:

$$E_r = (\phi_{r+h,z} - \phi_{r-h,z})/2h \quad (17)$$

$$E_z = (\phi_{r,z+h} - \phi_{r,z-h})/2h \quad (18)$$

The computer code was applied to study the plasma diode in various schemes, viz. cathode having 3 nozzle radial planes, 4 nozzle planes (Figures 2a and 3), 6 nozzle planes, etc. Also, corona discs having sharp spikes were located on either side of nozzle planes in some of the studies.

RESULTS AND DISCUSSION

Potential distributions and field variations inside the A-K gap were numerically computed using (16)-(18) for different gaps d and applied voltage ϕ_0 in the various schemes. Of these the potential distribution in the diode symmetric plane in Figure 3 for d = 10 mm and arbitrary ϕ_0 = 100, is plotted in same Figure 3. The potentials here show bumps around the nozzle pinnacles. It is seen that the bumps are highly peaked in smaller d cases and the respective radial electric fields as illustrated in Figure 4 are higher. As seen in Figure 4, E_r decreased exponentially with radial distance in general. A larger d here gave lesser field and tended to flatten the bumps in potential distribution while a smaller gap gave higher electric fields more than MV/m. For instance, for the 4-radial plane case in Figure 4 with ϕ_0 = 10 kV, the resulting electric fields over the cathode is around 6.2 x 10^6 V/m for d = 2 mm while it is 1.2x10^6 V/m for d = 25 mm. Figure 5 compares electric fields E_r in diodes having different cathode structures (a)-(e). It reveals that smaller

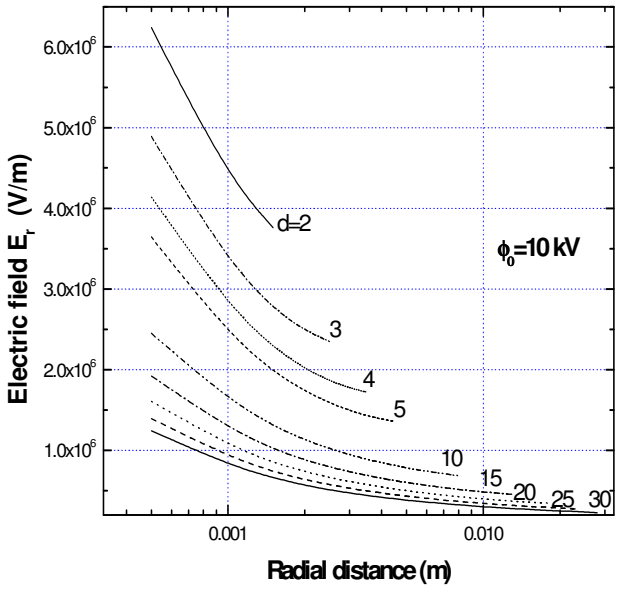

Figure 4. Electric field E_r variation with radial distance plotted for various A-K gaps in diode of Figure 2a with nozzle-planes separated 40 mm from each other.

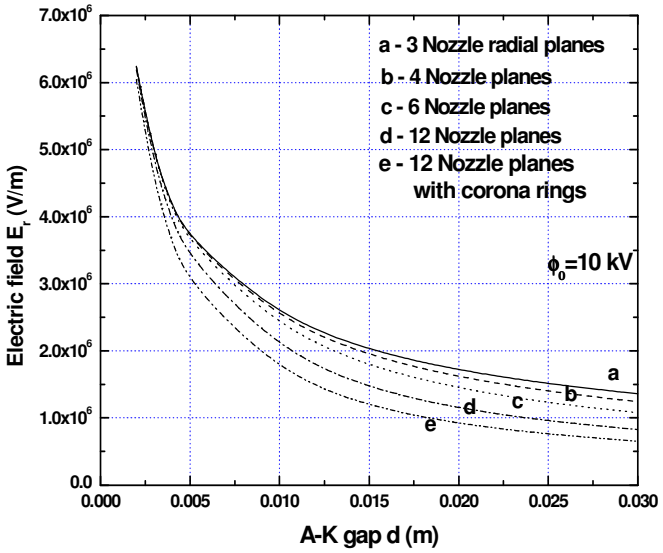

Figure 5. Electric field E_r over the cathode surface plotted against A-K gap d for various diodes geometries and different cathode definitions (a-e).

number of nozzle radial planes gave higher electric field. For instance, the field is almost 26% more in case of 3-nozzle planes as compared to the 12-nozzle planes with other things being same. Presence of corona ring spikes placed on either side of nozzle planes flattened the bumps more and lowered E_r, as in (e) of 12-nozzle plane case, a reduction of about 17% is noted. Maximum field emission current densities emitted from present cathode given by Equation (5) are tens of MA/m^2 for above electric fields of a couple of MV/m. The current however, reduced rapidly during transport inhibited by gas collisions abundant especially at the high pressures and consequently current reaching anode is either zero or negligibly small. In these conditions electron density attained over cathode through charge multiplication from (9) and (10) in diode of 4-nozzle-plane cathode were determined for various d from 2 to 30 mm. Of these, the results for d = 10, 20, 30 mm are only depicted in Figure 6. In these at the higher pressures over 200 Torr, (9) alone is active while at lower pressures (10) is active. Consequently for a pressure just below 100 Torr, electron density sharply increased to many orders and thereafter attained a plateau in the pressure range of 1-50 Torr caused by saturated multiplications. Electron density in this plateau for d=10 mm is ~ 4x10^{14} m^{-3} while same for d=2 mm is ~ 2x10^{15} m^{-3} as noted in another plot. For lower pressures below 1 Torr, as the gas densities are small the ions created as well as reaching the cathode are reduced giving negligible secondary electrons. This coupled with low gas density gave lower multiplications and a nearly constant n_e at the low pressures in Figure 6. As a result, the lower plateau on the left side in Figure 6 for the lower pressure range is solely due to the primary electrons.

Comparison of electron-density variation in different gaps in Figure 6 shows that the density is higher in both top and bottom plateaus for lower d due to higher multiplications in general. Curves of higher d are shifted to the lower pressure side due to same reasoning. Figure 7 compares the densities at different fields inside a given A-K gap of 10 mm and reveals the tendency of a higher density with increasing field. Here for the lower E_r cases, the top plateaus got constricted and steepened, and are shifted to the lower pressure side and gave reduced peaks. These observations revealed that higher electric field gave higher multiplications.

Figures 6 and 7 presume that current transported to anode is negligible or zero and so there is no heating of the corona. This cold corona of oxygen is ideal medium for breeding ozone. The binding energy of O_2 to be overcome to form O radicals as in (1) having cross section around 1.3x10^{-18} cm^2 (Tegeder et al., 2001) is provided by the electrons. O thereupon joins with free O_2 and forms O_3 as in (2) with cross sections about 3.7x10^{-17} cm^2 (Tegeder et al., 2001) and a release of energy equal to 1.06 eV. So the overall O_3 forming reactions made of (1) and (2) is endothermic and use a net energy of only 1.49 eV from the electrons. This means that a single electron of 10 keV in present cold corona is capable of producing tens of thousands of ozone forming reactions. So ozone density (n_{oz}) formed in this case is over 10^{19} m^{-3} for maximum electron densities available in Figures 6 and 7. n_{oz} could be even higher in the range 10^{19} -10^{21} m^{-3} by

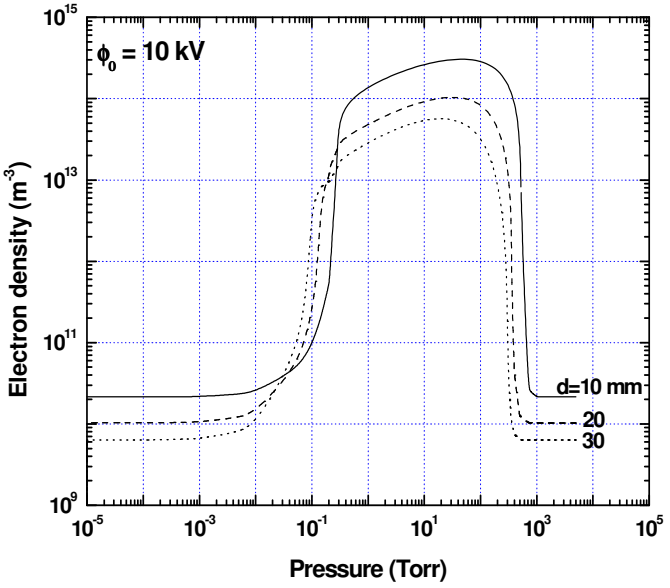

Figure 6. Results of field driven electron density multiplication over cathode vs. gas pressure compared for various A-K gaps d in diode of Figure 4.

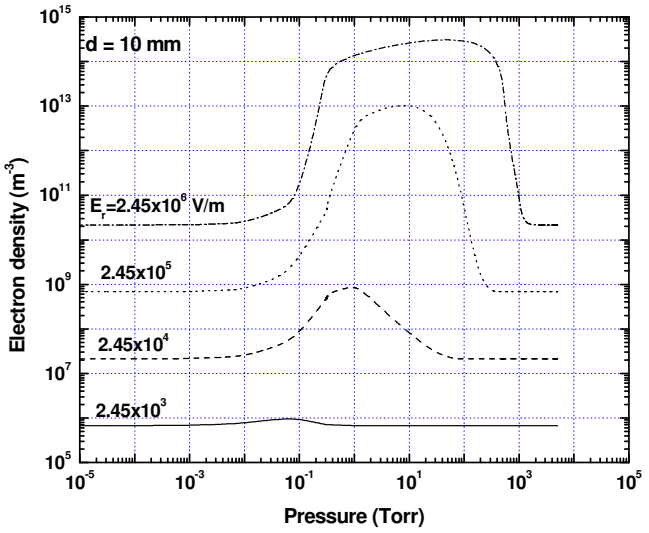

Figure 7. Electron density plotted against gas pressure for various electric fields E_r over cathode in diode of Fig. 4 with d=10 mm.

increasing electron energy and gas pressure suitably to a few times higher.

As stated earlier, a finite current I is transported in the corona in sub-Torr gas pressures and vacuum. The space-charge limited I for voltage ϕ_0 and d is written in the modified Child-Langmuir (Vijayan and Patil, 2008) form as:

$$I = 2.34x10^{-2} a\phi_0^{3/2} / [(d-x)^2 + R\phi_0^{1/2}] \quad (19)$$

Where $a = 2\pi r_A l$, r_A is anode radius, x is the corona plume depth, $R = \eta d / a$ is resistance offered by the neutral gas(Vijayan and Venkatramani, 2004; Patil and Vijayan, 2008) of density N_o, plasma resistivity $\eta = 7x10^{-7} T^{1/2} \frac{N_0}{n_e}$, and T the plasma temperature respectively. Resulting Joule heating inside corona is written as:

$$M_K S_K T + M_A S_A T + M_O S_O T + L_o = \phi_0 It \quad (20)$$

where M_K, M_A, and M_O are masses of the heat affected zones of cathode, anode, and gas respectively; S_K, S_A, and S_O similarly their specific heats, L_o is heat losses mainly due to convection and conduction (Patil and Vijayan, 2008), and t is time for attaining steady state temperature T. Estimations of (20) with I values of μA show that temperature rises are high only for d less than 5 mm and pressures less than 100 Torr. Temperatures in general are close to the ambient for A-K gaps of 10 to 30 mm and gas pressures ~1000 Torr. Plasma density n_e (Patil and Vijayan, 2008) in heated plasma in former cases is given by the corona model as:

$$n_e \approx 1.14025\ x10^5 N_0 \frac{(k_B T)^{3/4}}{(eV_i)^{11/4}} \exp(-eV_i / k_B T) \quad (21)$$

Where k_B is Boltzmann constant and V_i is ionization potential. For higher n_e with appropriate T such that, $\frac{n_e}{T^{1/2}} > 3x10^{13} V_i^3$, the Saha model is applicable and written as:

$$n_e \approx N_0 [2.4x10^{-4} \frac{T^{5/2}}{P} \exp(-eV_i / k_B T)]^{1/2} \quad (22)$$

Where gas pressure P is in Torr and T in eV. For the present low pressure and d windows, Figure 8 reveals that a heated corona is attained for T below 1150 K and thermally equilibrated plasma for T above 1400 K. The magnitudes of densities in Figure 8 however, are too small (10^2 - 10^6 m^{-3}) to make any noticeable difference to field induced densities depicted in Figures 6 and 7. In other words Figures 6 and 7 by and large describe the true density variations in present corona. Whereas plasma heating in the above window adversely affected ozone formation and aided rapid ozone reversal. They in turn resulted in reduction of ozone density at any given time. However, net ozone in the higher d and pressure windows were unaffected as there was no heating.

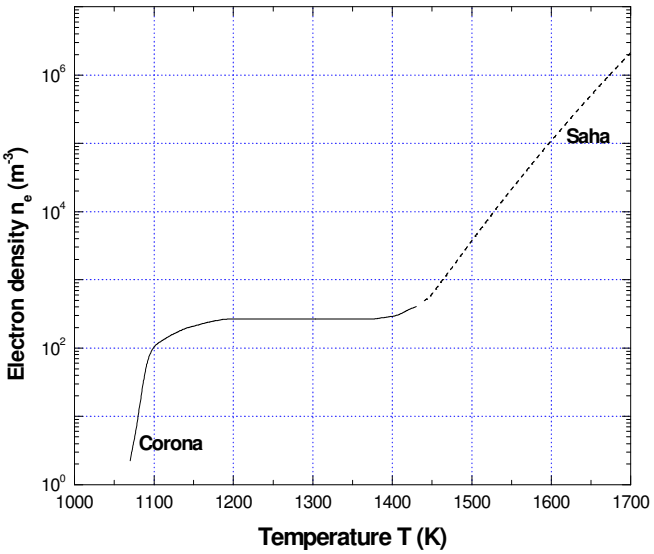

Figure 8. Current driven plasma density variation with temperature in small A-K gap regime of diode in Figure 4 at sub-Torr gas pressures.

Figure 9. Photograph of the ozone generator cum processor.

Generator development and experiments

The generator cum processor system was developed as per the schematic of Figure 2a and a photograph of the same shown in Figure 9. Ozone output generated in the generator and recorded in preliminary experiments is plotted against applied voltage in Figure 10. These plots are for a diode having A-K gap d=10 mm, 192 nozzles in 12 cathode radial planes on K-mast and for air pressures from1100 to 3000 Torr and measurements carried out by employing an electrochemical analyzer. The generator will now be characterized in detail and made available for the various applications. The maximum ozone dose plotted in Figure 10 is limited to100 ppm solely by the measuring device. Polynomial scaling of the values in Figure 10 at the higher voltages indicates ~10,000 - 20,000 ppm at 30 kV and ~100,000 - 200,000 ppm at 60 kV. For measurement of these doses and confirmation, suitable UV based analyzers are being procured. The above doses are with air as test gas. With oxygen input, the ozone output is expected to be still higher by five times.

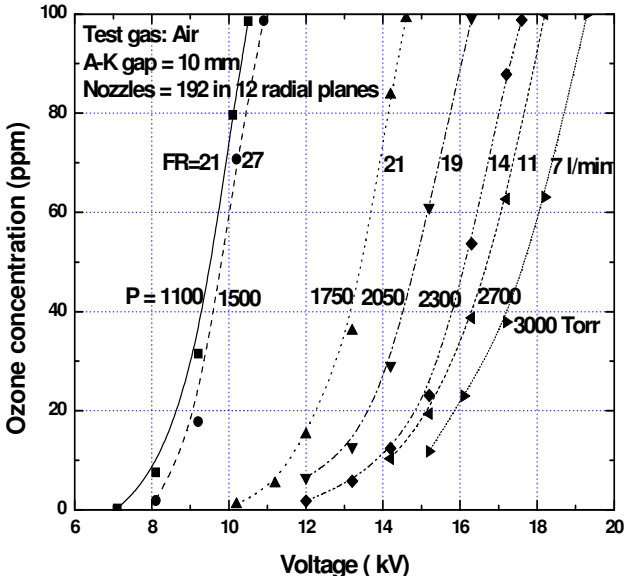

Figure 10. Ozone concentration vs. voltage recorded by electrochemical analyzer in various conditions of air pressure and flow rate (FR).

CONCLUSIONS

Corona plasma formation in an electric field driven ozone generator diode towards genesis of ozone has been investigated and characterized in theory. Ozone is formed in a cold corona plasma regime inside the plasma diode made of a novel cathode assembly which is coaxially placed inside the anode cup and pervaded in oxygen gas. The cathode-assembly design here is made of large number of gas nozzles arranged symmetrically on number of radial planes on the axial tubular cathode-mast which also admitted oxygen gas in to the A-K gap. An r-z five-point finite-difference scheme using successive over-relaxation has been devised in MATLAB code to numerically study the potential and electric field distributions in different diode configurations. The sharp endings on the nozzles created peak electric field ~10^6-

10^7 V/m over the cathode surface in the form of bumps and caused field emissions that aided formation of intense oxygen corona plume. For higher pressures above 200 Torr overwhelmed by gas collisions, primary ionizations alone support electron multiplication in corona in view of which neither electron current nor ion current transported. At the low pressures however both primary and secondary electrons took part in the ionizations. The resulting peak electron density in corona was in the range 10^{14} – 10^{15} m^{-3} but reduced and shifted to the lower pressure side in larger A-K gaps while the density increased with higher fields and smaller gaps. In these conditions resulting cold plasma offered a fertile medium for ozone genesis. With the evolution of space charge limited currents at the extremely low pressures and small A-K gaps, the resulting joule heating however inhibited ozone production.

The results indicate that larger A-K gaps give lower electric field and smaller currents resulting in negligible heating. This produced a cold negative corona favorable for copious amount of ozone formation. The same is presently fulfilled by optimizing the applied voltage, A-K gap distance, gas pressures and cathode configuration. A cold corona obtained this way in wide anode-cathode gaps of 10 - 30 mm pervaded by oxygen at pressures less than 10^3 Torr could give ozone density over 10^{19} m^{-3}. The generator so developed, gave ozone in hundreds of ppm in preliminary experiments limited only by analyzers employed. The generator will now be characterized in higher concentrations using higher order analyzers. Ozone will then be employed for the various important applications, such as, ozone therapy, purification of ambient air and drinking water.

ACKNOWLEDGEMENTS

The authors thank Dr. K M Vasudevan Pillai, Secretary and CEO, Mahatma Education Society (MES) and Dr. (Mrs.) Daphne Pillai, Joint Secretary and Rector, MES for the encouragements; Dr. A K Das, Head, L and PTD, BARC for discussions and Department of Science and Technology (DST) Government of India for supporting the work. The authors also thank Library staff of PIIT for support in the computation facilities.

REFERENCES

Kogelschatzt U, Eliasson B, Egli W (1999). “From ozone generators to flat televisionsreens: history and future potential of dielectric barrier discharges”, October Pure Appl. Chem., 71: 1819-1828.

Renner RC, Robson MC, Miller GW, Hill AG (1988). “Ozone in water treatment – The Designer’s role”, Ozone Science Eng., 10 (1): 55-87.

Vijayan T, Patil JG (2008). “High-tension corona controlled ozone generator for environment protection”, in Proc. 23rd National Sym. Plasma Science and Technology pp 318-320. (PLASMA-2008), BARC, December, 10-13.

Jen-Shih C (1991). “Corona discharge processes”, IEEE Trans. Plasma Sci., 19(6): 1152-1166.

Kitayama J, Kuzumoto M (1997). “Theoretical and experimental study on ozone generation characteristics of an oxygen-fed ozone generator in silent discharge”, J. Phys. D: Appl. Phys., 30: 2453-2461.

Yagi S, Tanaka M (1979). “Mechanism of ozone generation in air-fed ozonisers” J. Phys. D: Appl. Phys., 12:1509-1520.

Dekowski J, Mizeraczyk J, Kocik M, Dors M, Podilinski J (2004). “Electro-hydrodynamic flow and effect on ozone transport in corona radical shower reactor”, IEEE Trans. Plasma Sci., 32(2): 370-379.

Vijayan T (2006). “Electric field-emission model of corona discharge in an ozone generator”, in Proc. DAE-BRNS-PSI Sym. Electron Beam Transport and Applications (SEBTA-06), BARC, pp. 264-268. September.

Pekarek S, Rosenkranz J, Kriha V (2000). “Ozone generation in gas flow enhanced hollow needle to plate electrical discharge in air”, Czech. J. Phys., 53(3): 385-388.

Kireeff M, Covo MA, Friedman A, Westenskov G, Barnard JJ, Cohen R, Seidl P, Kwan JD, Logan G, Baca D, Bieniosek F, Celata CM, Vay JL, Vujic JL (2006). “Beam Energy Scaling of Ion-Induced Electron Yield from K^+ Impact on Stainless Steel”, Lawrence Livermore National Laboratory UCRL-JRNL–219620 Physical Review Special Topics–Accelerator and Beams, Mar. vol. 4.

Vijayan T, Venkatramani N (2004). “Heating and Transport of Metal Plasma in a Vacuum-Arc Rail Gun”, IEEE Trans. Plasma Sci., April, 32(2): 770-774.

Vijayan T (1999). “Nine-point simplified variable-mesh finite-difference formulation of Poisson’s equation”, Nucl. Instrum. Methods A., 427: 437-439.

Lyshevsk SE (2003). Engineering and Scientific Computations using MATLAB, New Jersey: John Wiley and Sons, 2003.

Davis JCh, Anderson NE, Ramirez JG, Enneking FK, Meisel MW (2007). “Finite Difference Modeling of the Anisotropic Electric Fields generated by Stimulating Needles used for Cathetar Placement” IEEE Trans. Biomed. Eng., 54(7): 1186-1190.

Tegeder P, Kendall PA, Penno M, Mason NJ, Illenberger E (2001). “Electron stimulated desorption of O^- and O_2^- from condensed ozone: Possible implications for the heterogeneous photochemistry of stratospheric O_3”, Phys. Chem. Chem. Phys., 3: 2625-2629.

Patil JG, Vijayan T (2008). “Modeling and characterization of field-enhanced corona discharge in ozone-generator diode”, in Proc. 23rd National Sym. Plasma Science and Technology (PLASMA-2008), BARC, December. 10-13, 2008, pp. 320-324.